Supporting Information

An Erythrocyte Membrane Coated Mimetic Nano-platform for Chemo-Phototherapy and Multimodal Imaging

Feng Xiao[1#], Jialong Fan[1#], Chunyi Tong[1#], Chang Xiao[1], Zhou Wang[1], Bin Liu[1]*, Muhammad Daniyal[2], Wei Wang[2]*

[1] *College of Biology, Hunan University, Changsha, 410082, China*

[2]*TCM and Ethnomedicine Innovation & Development International Laboratory, Innovative Materia Medica Research Institute, School of Pharmacy, Hunan University of Chinese Medicine, Changsha, 410208, P.R China.*

# These authors contributed to the work equally and should be regarded as co-first authors.

* To whom correspondence should be addressed. Tel: +86-731-89720939; Fax: +86-731-89720939;

E-mail: binliu2001@hotmail.com (B Liu),wangwei402@hotmail.com (W Wang)

Table of Contents

1. Experimental procedures

1.1 Materials

$K_3[Fe(CN)_6]\cdot 3H_2O$ was purchased from Fuchen Chemical Reagent Factory (Tianjin, China). Poly (N-vinylpyrrolidone) (PVP) was purchased from Zhanyun Chemical Co., Ltd. (Shanghai, China). Doxorubicin (DOX), folic acid (FA), MTT assay kit and dialysis bag were obtained from Solarbio Technology Co., Ltd. (Beijing, China). Rhodamine B was obtained from Biotopped Biotach (Beijing, China). N-Hydroxysuccinimide (NHS) and 1-ethyl-3-(3-dimethylaminopropyl) carbodiimide (EDC) were purchased from Sigma-Aldrich (St Louis, MO, USA). ICG was purchased from Heowns Biochemical Technology Co., Ltd. (Tianjin, China). DSPE-PEG2000-NH2 and FITC-PEG2000-DSPE were obtained from Pengsheng Biotech (Shanghai, China). Hochest-33342 and calcein acetoxymethyl ester (Calcein AM)

were bought from Yeasen Biotechnology (Shanghai, China). Annexin V Cell Apoptosis Analysis Kit was obtained from Sungene Biotech Co., Ltd. (Tianjin, China). Dulbecco's Modified Eagle's Medium (DMEM) was purchased from HyClone. All used cell line was purchased from the cell library of Xiangya Central Laboratory, Central-South University (Changsha, China). BALB/c mice were obtained from Hunan Silaike experimental animal Co. Ltd. All other reagents were of analytical purity and used without further purification.

1.2 Methods

Scanning electron microscopy (SEM) images were performed on a JSM-6700F (JEOL, Japan) instrument at 5.0 kV accelerating voltage. The morphology of SCPB NPs and SCPB@RBC NPs was examined by Transmission electron microscope (TEM) (JEOL, JEM-2100F, 200 kV). After degassing was performed under vacuum condition at 40 °C for 60 h, N_2 adsorption-desorption isotherms were measured by a fully automatic specific surface area and pore size analyzer (NOVA1000e, Quantachrome, USA). Wide-angle XRD measurement by X-ray diffractometer (D8 Advance, BRUKER, Germany) to detect the phase purity of samples. The FT-IR spectra were recorded on a Nicolet 6700 FTIR spectrophotometer (Thermo Fisher Scientific Inc, USA). UV-Vis absorption was measured on a DU800 spectrophotometer (Beckman Coulter Inc, USA). The optical density (OD) was measured with a microplate reader (EnSpire 2300, PerkinElmer, Singapore). Zeta potential analysis and dynamic light scattering (DLS) were determined using a Zetasizer (Malvern Nano series, Malvern, UK). The photothermal property of the material was measured using a fiber-coupled continuous semiconductor laser (808 nm, Changchun Leishi Optoelectronics Technology Co., Ltd., China) and the temperature was monitored with a thermal infrared imaging camera (Flir C2, USA). Iron concentration was measured with an inductively coupled plasma-optical emission spectroscopy (ICP-OES, Perkin-Elmer model 3300 XL, USA). All fluorescence images were obtained on a confocal laser scanning fluorescence microscope (CLSM) (FV1200, Olympus, Japan). Apoptosis rates were quantified by flow cytometry (CytoFLEX, Beckman, USA). The hematoxylin & eosin (H&E) and TUNEL-stained slices were observed with a fluorescent inverted microscope (IX73, Olympus, Japan).

1.3 Calculation of the molar extinction coefficient

The molar extinction coefficient (ε) is an important index for evaluating the light absorption performance of a material. If the molar extinction coefficient of a material is higher, the light absorption and heat conversion capacity of material will be higher.[1]

The extinction coefficient can be calculated as equation (1)

$$\varepsilon = (A V_{NC} P N_A) / (L C_{wt}) \quad (1)$$

Where: ε ($cm^{-1} \cdot mol^{-1} \cdot L$) is the molar extinction coefficient. A is the light absorption intensity of the nanomaterials in the near-infrared region, and V_{NC} (cm^3) is the average volume of the nanoparticles. ρ (g cm^{-3}) is the density of nanometers, the density of HMPB NPs is 1.8 g cm^{-3}, and N_A (6.0 2×10^{23}, mol^{-1}) is the Avogadro constant. L is the path-length (1 cm), and C_{wt} (g mL^{-1}) is the mass concentration of the nanomaterials.

According to equation (1), the molar extinction coefficient of PB nanomaterials can be approximated as equation (2).

$$\varepsilon = A V_{NC} \times 5.418 \times 10^{28} \quad (2)$$

Where: ε (cm-1·mol-1·L) is the molar extinction coefficient. A is the light absorption intensity of the nanomaterials in the near-infrared region, and V_{NC} (cm^3) is the average volume of the nanoparticles.

Table S1 Size, volume, absorption value and molar extinction coefficient of different HMPB NPs

Morphology	Particle size/nm	10^{15} Volume cm^{-3}	10^{-13} ε	A	10^{-13} ε
Spheric	150(diameter)	1.7663	9.5695A	1.220	1.1675
Cubic	150(side length)	3.3750	1.8286A	1.532	2.8014

It can be seen from table S1 that the molar extinction coefficient of the cubic HMPB NPs is larger than the spheric HMPB NPs.

1.4 Calculation of the photothermal conversion efficiency

Photothermal conversion efficiency (η) is also an important indicator that directly reflects the photothermal performance of nanomaterials. The photothermal conversion efficiency of HMPB NPs is determined according to the previous method.[2] Detailed calculation was given as follows:

Based on the total energy balance for this system:

$$\sum_i m_i C_{p,i} \frac{dT}{dt} = Q_{NPs} + Q_s - Q_{loss} \quad (3)$$

Where m and C_p are the mass and heat capacity of water, respectively. T (°C) is the solution of temperature, Q_{NPs} is the energy inputted by HMPB NPs, Q_s is the baseline energy inputted by the sample cell, and Q_{loss} is heat conduction away from the system surface by air.

$$Q_{NPs} = I(1 - 10^{-A_\lambda})\eta \quad (4)$$

Where I is the laser power, A_λ is the absorbance of HMPB NPs at the wavelength of 808 nm, and η is the conversion efficiency from the absorbed light energy to thermal energy.

Qs is the heat associated with the absorbance of the solvent, and the pure water containing no HMPB NP is independently measured to be 0.

Q_{loss} is thermal energy lost to the surroundings:

$$Q_{loss} = hA\Delta T \quad (5)$$

Where: h is the heat transfer coefficient, A is the surface area of the container, and ΔT is the temperature change, which is defined as T-T_{surr} (T and T_{surr} are the solution temperature and ambient temperature of the surroundings, respectively.)

At the maximum steady-state temperature, the heat input is equal to the heat output, that is:

$$Q_{NPs} + Q_s = Q_{loss} = hA\Delta T_{max} \quad (6)$$

Where ΔT_{max} is the temperature change at the maximum steady-state temperature. According to the equation (4) and equation (6), the photothermal conversion efficiency (η) can be determined:

$$\eta = \frac{hA\Delta T_{max} - Q_s}{I(1 - 10^{-A\lambda})} \quad (7)$$

In this equation, the only hA is unknown for calculation. In order to get the hA, we herein introduce θ, which is defined as the ratio of ΔT and ΔT_{max}:

$$\theta = \frac{\Delta T}{\Delta T_{max}} \quad (8)$$

Substituting equation (8) into equation (3) and rearranging equation (3):

$$\frac{d\theta}{dt} = \frac{hA}{\sum_i m_i C_{p,i}}\left[\frac{Q_{NPs} + Q_s}{hA\Delta T_{max}} - \theta\right] \quad (9)$$

When the laser was shut off, the $Q_{NPs} + Q_s = 0$, equation (9) changed to:

$$dt = -\frac{\sum_i m_i C_{p,i}}{hA}\frac{d\theta}{\theta} \quad (10)$$

Integrating equation (10) gives the expression:

$$t = -\frac{\sum_i m_i C_{p,i}}{hA}\ln\theta \quad (11)$$

Thus, $\frac{\sum_i m_i C_{p,i}}{hA}$ can be determined by the linear relationship of time versus $-\ln\theta$. Compared with solvent (water, 2×10^{-3} Kg), the mass of NPs (2×10^{-7} Kg) was too little. Generally, the specific heat of water is much higher than other materials.

Consequently, the m_{NPs} and $C_{p,NPs}$ of NPs were neglected. m_{H_2O} was 2 × 10^{-3} Kg. C_{p,H_2O} was 4.2 × 10^3 J Kg^{-1} °C.

Table S2 Specific value of HMPB NPs with different morphologies

Morphology	A_{808}	ΔT_{max} / °C	τ_s	hA	η (%)
Spheric	0.971	15	259.17	0.0142	47.75
Cubic	1.042	13.9	346.87	0.0121	37.03

It can be seen from Table S2 that the photothermal conversion efficiency of spherical HMPB NPs is better than the cubic HMPB NPs.

2. Supplementary Figures

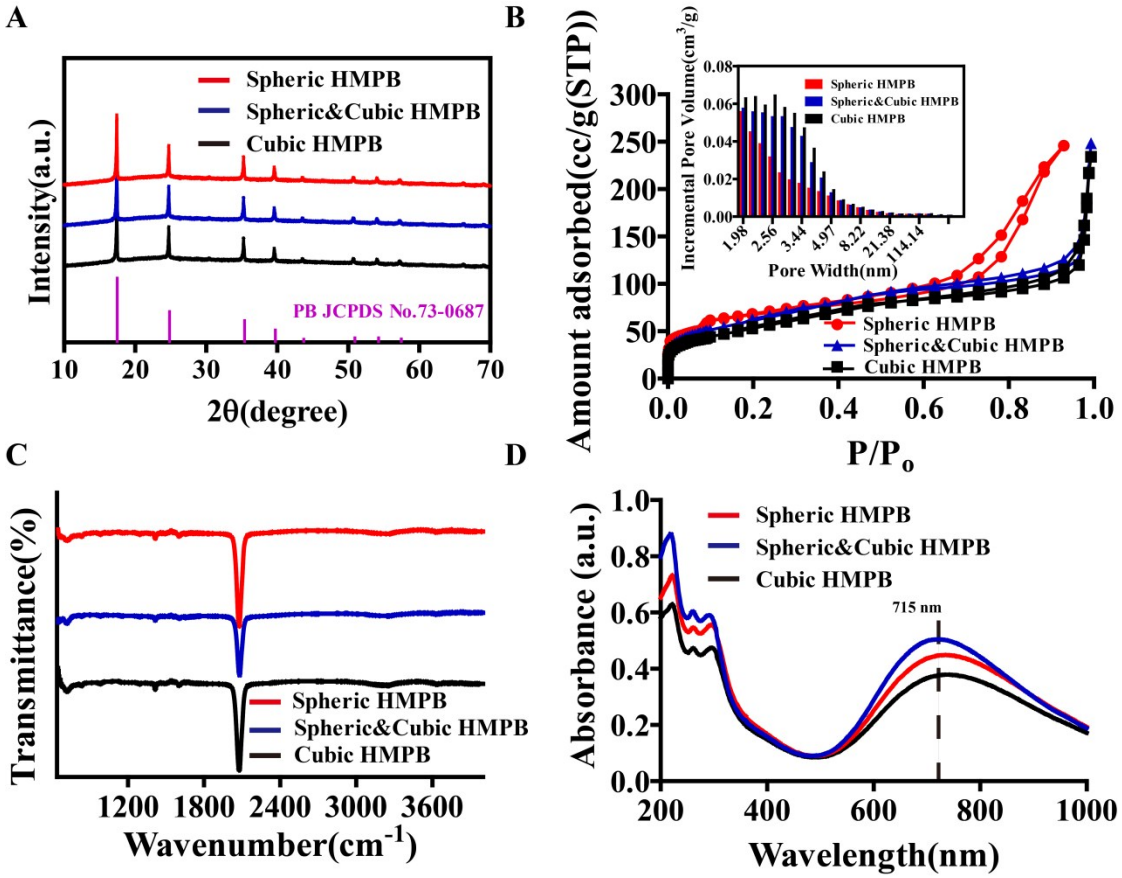

Fig. S1. (A) XRD patterns of spheric, spheric & cubic and cubic HMPB NPs. (B) N2 adsorption−desorption isotherms of spheric, spheric & cubic and cubic HMPB NPs; the inset was their corresponding pore size distribution profile. (C) FTIR spectra and (D) UV-Vis absorption spectra of spheric, spheric & cubic and cubic HMPB NPs.

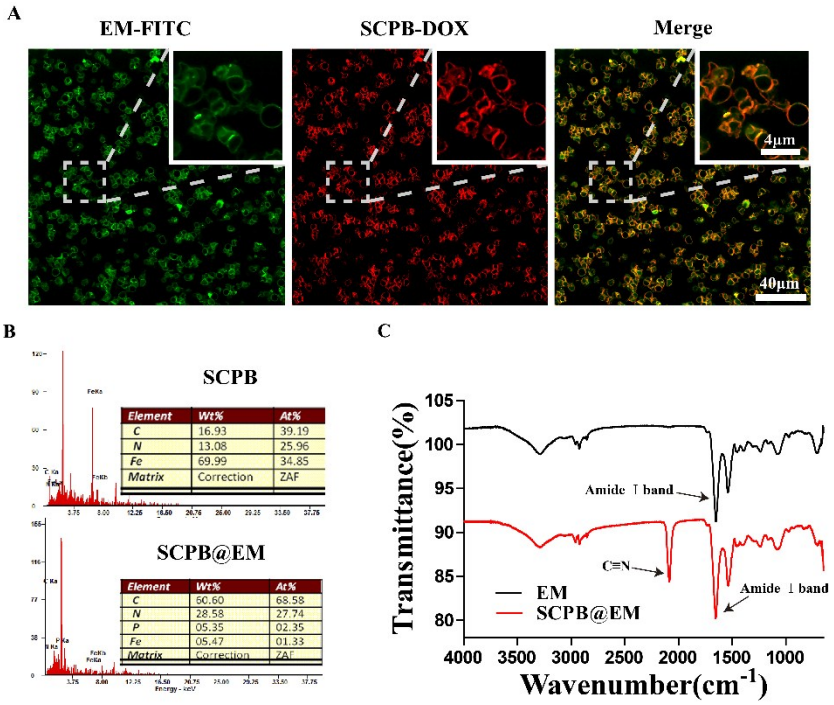

Fig. S2. (A) Confocal fluorescent microscopy images of the SCPB@DOX@EM NPs (RBC membrane labeled with FITC emitted green fluorescence, SCPB@DOX NPs showed red fluorescence, scale bar = 40 μm. Inset: scale bar = 4 μm). The EDS (B) and FT-IR spectra (C) of SCPB and SCPB@EM NPs. Peaks of SCPB@EM NPs at 2086 cm^{-1} and 1680 cm^{-1} could be attributed to C ≡ N and Amide I band, respectively.

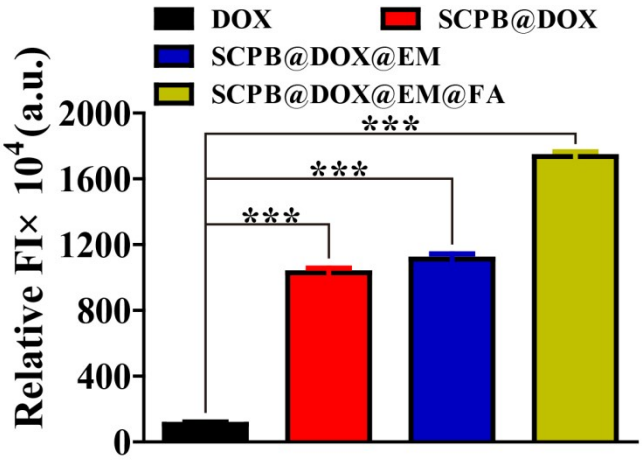

Fig. S3. Relative fluorescence intensity analysis of HeLa cells after with DOX, SCPB@DOX, SCPB@DOX@EM and SCPB@DOX@EM@FA treatment (P value: *** $p < 0.001$).

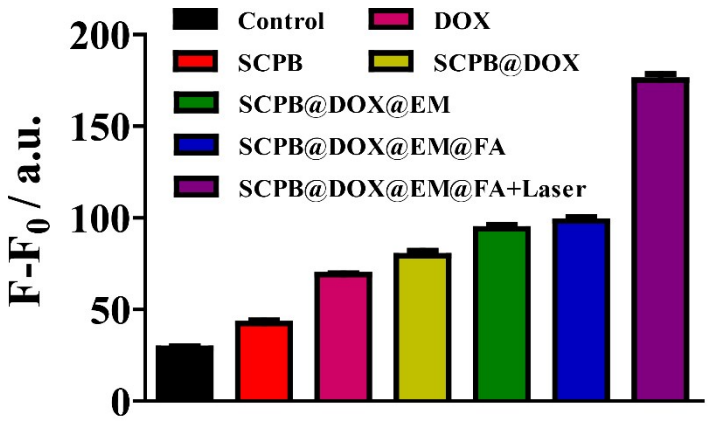

Fig. S4. Fluorescent monitoring of DOX, SCPB@DOX, SCPB@DOX@EM, SCPB@DOX@EM@FA, SCPB@DOX@EM@FA+Laser induced-Cyt c release in HeLa cells.[3]

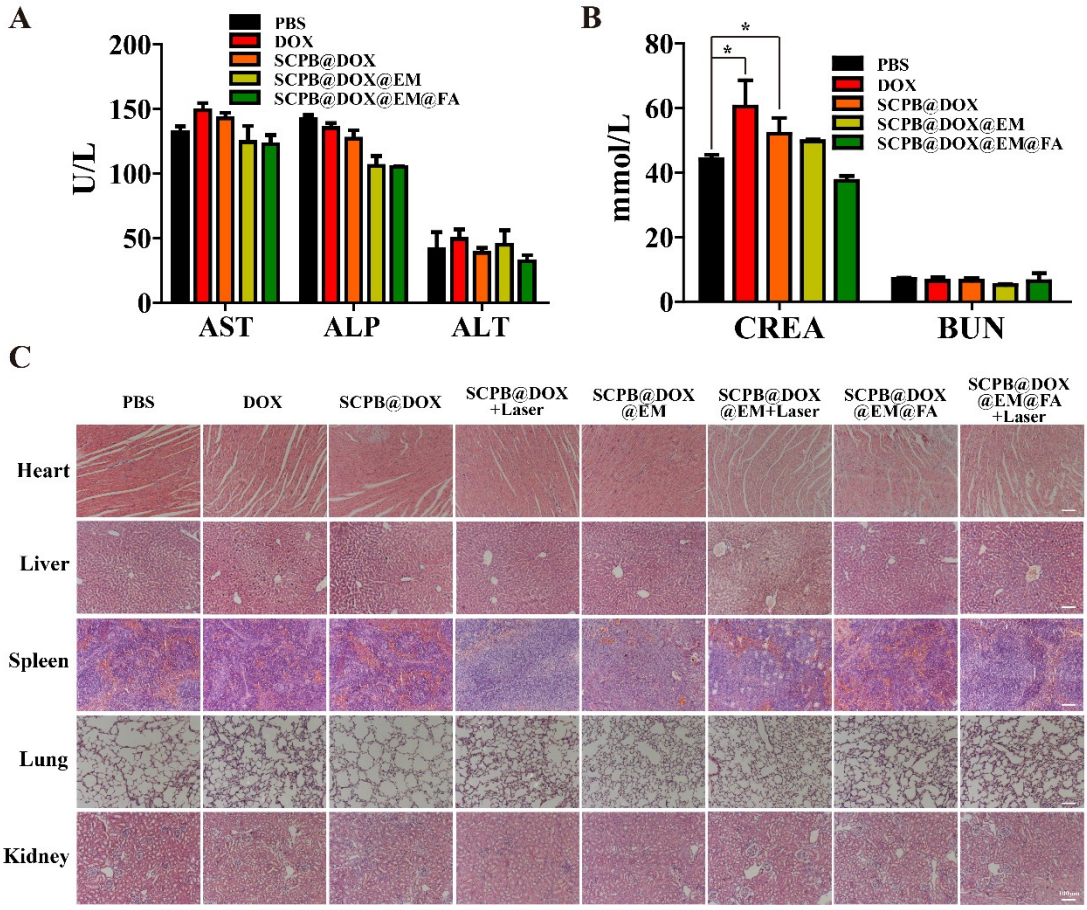

Fig. S5. (A). Hepatotoxicity and (B) nephrotoxicity analysis. (C) H&E staining of heart, liver, spleen, lung, and kidney tissue slices from tumor-bearing mice receiving different treatments for 16 days. (with NIR laser: 808 nm, 0.8 W cm^2) (scale bar = 100 μm). Data are shown as mean standard deviation (SD), n=3. (P value: * $p < 0.05$).

References

1 Zhao Y, Pan H, Lou Y, Qiu X, Zhu J, Burda C. Plasmonic Cu_2− x S nanocrystals: optical and structural properties of copper-deficient copper (I) sulfides. Journal of the American Chemical Society 2009;131:4253-61.

2 Roper DK, Ahn W, Hoepfner M. Microscale heat transfer transduced by surface plasmon resonant gold nanoparticles. The Journal of Physical Chemistry C 2007;111:3636-41.
3 Qin Y, Daniyal M, Wang W, Jian Y, Yang W, Qiu Y, et al. An enhanced silver nanocluster system for cytochrome c detection and natural drug screening targeted for cytochrome c. Sensors and Actuators B: Chemical 2018.